

Article

Experimental Investigation of the Supercavitation and Hydrodynamic Characteristics of High-Speed Projectiles with Hydrophobic and Hydrophilic Coatings

Huixia Jia ^{1,*},[†] , Rishan Xie ^{1,†} and Yangjie Zhou ²

¹ National-Provincial Joint Engineering Laboratory for Fluid Transmission System Technology, Zhejiang Sci-Tech University, Hangzhou 310018, China

² Ningbo Sunny Instruments Co., Ltd., Ningbo 315400, China

* Correspondence: huixia.jia@zstu.edu.cn

† These authors contributed equally to this work.

Abstract: Supercavitation technology has important application value in military and national defence fields because of its huge potential in drag reduction, while the cavitation around underwater moving objects may be affected by the surface properties of objects. In this paper, the supercavitation characteristics and hydrodynamics of a projectile with hydrophobic and hydrophilic surface coatings were experimentally studied using a high-speed camera. The supercavitation evolution, cavitation size, velocity change, drag force coefficient, and ballistic deflection of projectiles in different water depths are compared and analyzed. The results show that the length and diameter of the supercavity increase with the decrease in water depth. At the same water depth and cavitation number, the length and diameter of the supercavitation of the projectile with hydrophobic coating were greater than those of the projectile with hydrophilic coating, and the drag force coefficient of the hydrophobic projectile was obviously smaller than that of the hydrophilic projectile. Under the working conditions of 6.67D, 16.7D, and 33.3D, the drag force coefficient of the hydrophobic projectile could be reduced by about 20–40% compared with that of the hydrophilic projectile. The maximal reduction in drag force coefficient was up to 40% at $\sigma = 0.34$ under a water depth of 33.3D. The velocity attenuation of hydrophobic projectile was about 20% slower than that of hydrophilic projectile. In addition, the ballistic stability of hydrophobic coated projectiles was better than that of hydrophilic coated projectiles in the different water depths observed in the paper.

Keywords: supercavitation; hydrodynamics; hydrophobic; hydrophilic



Citation: Jia, H.; Xie, R.; Zhou, Y. Experimental Investigation of the Supercavitation and Hydrodynamic Characteristics of High-Speed Projectiles with Hydrophobic and Hydrophilic Coatings. *Fluids* **2022**, *7*, 363. <https://doi.org/10.3390/fluids7120363>

Academic Editor: Mehrdad Massoudi

Received: 7 October 2022

Accepted: 15 November 2022

Published: 23 November 2022

Publisher's Note: MDPI stays neutral with regard to jurisdictional claims in published maps and institutional affiliations.



Copyright: © 2022 by the authors. Licensee MDPI, Basel, Switzerland. This article is an open access article distributed under the terms and conditions of the Creative Commons Attribution (CC BY) license (<https://creativecommons.org/licenses/by/4.0/>).

1. Introduction

Cavitation is a common phenomenon in nature. In industrial engineering, the phenomenon can also occur in propulsion systems such as pumps, hydrofoils, or marine propellers. When cavitation wraps around a body, the phenomenon is called supercavitation. Supercavitation technology has important applications in national defence and military fields, such as supercavitating torpedoes and projectiles.

Over the past few decades, the supercavitation flow has been studied by many researchers. The research of Logvinovich [1] established the theoretical basis for supercavitation calculation, which can be used for high-speed torpedo design. Waugh and Stubstad [2] collected detailed experimental data on the supercavitation flow and water ballistics of missiles in and out of water carried out by the US Navy. Their experimental velocity and cavitation number ranged from 16.15 to 19.20 m/s, and 0.045 to 0.567, respectively, covering various flow states from full wet to full supercavitation. Vlasenko [3] disclosed some technical details of three sets of experimental equipment for realizing supercavitation with velocities ranging from 50 to 1300 m/s.

Hrubec [4] carried out a supercavitation experiment by using an underwater artillery device. Velocity was approaching or exceeding the speed of sound in water by 1.5 km/s. They found that ultrahigh-speed cavitation is prone to instability and may affect the trajectory of a blunt body.

Shi et al. [5] experimentally observed the phenomenon of supercavitation flow when high-speed projectiles vertically enter the water. They found that a shock wave forms and then propagates when the projectile hits the water surface. With the downward movement of the projectile, the tail of the supercavitation collapses, and at this time a secondary shock wave appeared.

When an object moves underwater near a free surface, the influence of the free surface on cavitation must be considered. On the basis of linearization theory, Franc and Michel [6] studied the effect of immersion depth on supercavitation length. Using ideal fluid theory, Amromin [7] performed supercavitation analysis in shallow water, taking into account the effects of the free surface and the rigid boundary on supercavitation flow. The calculation results show that the combination of effects leads to an increase in the cavitation number for a fixed-length cavity, and causes the 3D deformation of the cavity in a cross-section and the expansion of the lower cavity portion.

Faltinsen and Semenov [8] theoretically analyzed the steady cavitation flow of a hydrofoil under the effect of free surface and gravity, and gave an analytical solution of the cavitation flow field. Their results show that, as the hydrofoil approached the free surface, the cavity and free surface shapes changed. Both the free surfaces and gravity can decrease the cavity length.

Wang et al. [9] numerically investigated the natural cavitation around an axisymmetric projectile near a free surface using LES and the VOF method. They found that the cavity evolution on the upper side of the projectile was significantly different under the free surface effect than that at the lower side. On the upper side, the cavity grew slowly, the velocity of reinjection was higher, and the collapsed position of the cavity was closer to the main cavity.

Shi et al. [10] experimentally studied the evolution of supercavitation of various projectiles with different aspect ratios at different water depths using high-speed photography. They found that the size of the cavitation increased with a decrease in water depth, and a vertical water fin appeared on the free surface when the projectile moved near the free surface under a water depth of 3.33D.

In recent years, the effect of hydrophobic characteristics on the drag reduction was examined by many researchers [11–16]. However, in their studies, the cavitation phenomenon was not considered. There are relatively few studies on the influence of surface properties on cavitation flow.

Some studies about the hydrophobic effect on cavitation flow focus on the low-speed flow of underwater objects. Leger and Ceccio [17] investigated noncavitating and cavitating flows around hydrophilic and hydrophobic spheres and cylinders. They found that the material properties strongly affected the shape of the cavity near the detachment.

A cavitating NACA0015 foil in three different tunnels was observed by Kawakami et al. [18]. They revealed remarkably different cavity shedding appearances and behaviors. They argued that surface effects could have a significant influence on the fully wetted time during cavity shedding. However, the results of most current studies do not agree, and the mechanism of cavitation is not completely understood.

Kim and Lee [19] numerically investigated the effect of the hydrophobic property on the cloud cavitation. Their results show that, as slip strength grew, the cavity was elongated, and the shedding frequency decreased. That means that cloud cavitation instability was alleviated as the hydrophobicity increased.

Mineshima et al. [20] studied the effects of hydrophilic and hydrophobic coatings on the characteristics of cavitation and flow field around hydrofoils using high-speed camera and laser Doppler velocimetry (LDV). Their results showed that the hydrophilic coating inhibited the inception and growth of the cavitation. In addition, the downstream

pressure fluctuation of the hydrofoil with hydrophilic coating was restrained under a certain cavitation number. The experimental investigation of Onishi et al. [21] also found that the cavitation inception number of the hydrophilic coating was lower than that of a hydrophobic coating.

Some studies regarding the effect of hydrophobic surfaces focused on the process of water entry. Ueda et al. [22] experimentally studied the water-entry of superhydrophobic low-density spheres. They found that the shape of the cavity pinch-off of low-density spheres was inconsistent with the shape of high-density spheres observed by Duclaux et al. [23].

Aristoff and Bush [24] studied the water entry of hydrophobic spheres at a certain contact angle with various impact velocities and sphere diameters. Their extensive dataset showed that cavities formed at all impact velocities had four distinct shapes defined by their collapse or pinch-off locations appearing at a specific location on the Bond–Weber diagram. On this basis, Speirs et al. [25] studied the water entry of spheres with different contact angles, and found that the shape of the cavitation during water entry was not only related to the Bond and Weber number, but also depended on the contact angle.

Zhang et al. [26] experimentally investigated the development and shedding mode of the cavitation for hydrophobic steel balls with different diameters and different impact velocities of water entry. The dependence of the two shedding modes on the Weber and Bond numbers was determined.

Li et al. [27] numerically investigated the cavity dynamics of a rotating hydrophobic sphere during its entry into the water. In their numerical simulation, the wettability of the sphere surface was realized with the dynamic contact angle, the boundary data immersion method (BDIM) was used to simulate the solid/fluid interaction, and the interface between liquid and gas was tracked with the volume-of-fluid (VOF) method.

Güzel and Korkmaz [28] experimentally studied the influence of hydrophobicity on free surface elevation and impact load during water entry of wedges and cones with different deadrise angles. They found that the jets, accumulations, and formation of cavities changed when objects with constant deadrise angles entered the water under the hydrophobic effect. The measured value of bumping load coefficient under hydrophobic effect could be reduced by 10–25% compared with that of a hydrophilic surface. In addition, Guzel and Korkmaz [29] experimentally investigated the water exit of partially and fully immersed spheres and flat plates with or without hydrophobic coatings using a high-speed camera and strain gauges. They found that the separation time of the water from the object occurred earlier due to the hydrophobic effect, that is, the pinch-off time of the fluid was earlier. The height of the water column behind the object was also smaller. In addition, they found that, when the surface of the object was uncoated, the strain measurements were repeatable under the same test conditions; however, when the surface was coated, the strain characteristics under the same test conditions were different. Therefore, they thought that similar experiments with different geometries such as cylinders are necessary to be carried out before conclusions are drawn on the effect of hydrophobicity of the water-exit process.

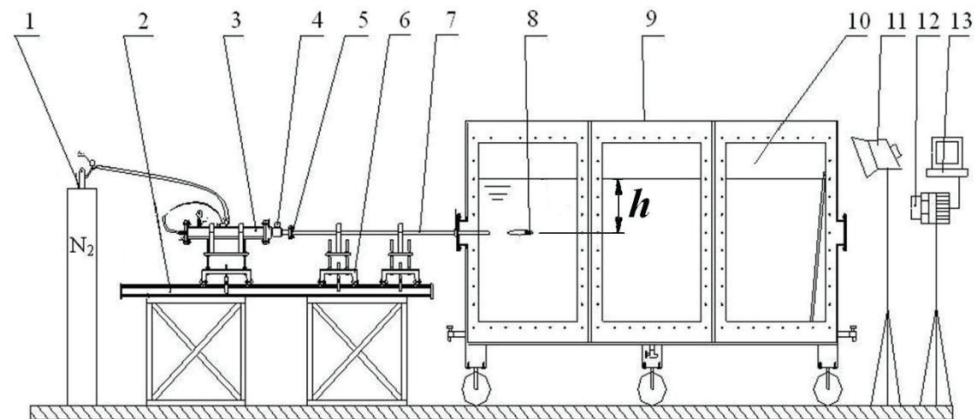
In summary, most previous studies focused on drag reduction in hydrophobic coatings without cavitation. Some researchers also studied the influence of surface coating properties on the flow of water entry or exit, or the cavitation flow around the hydrofoil. All these studies were aimed at low velocity flow. However, there is no relevant research about the influence of surface coating on the supercavitation flow characteristics of high-speed objects underwater and near a free surface.

In this paper, the supercavitation flow of high-speed projectiles with different surface coatings is experimentally investigated under the conditions of different water depths. The influence of surface coating on supercavitation flow and hydrodynamic characteristics of the projectiles is analyzed.

2. Experimental Setup and Methods

Figure 1 is the schematic diagram of the experimental setup used in this paper. On this experimental device, both supercavitation experiments of horizontally launched projectiles

at different water depths and water-entry/exit experiments at different angles could be carried out. A self-designed one-stage light gas gun was used to accelerate projectiles. The projectile was pushed by the high-pressure nitrogen in high-pressure chamber 3, accelerated in launch tube 7 to a certain velocity, and entered observation water tank 9. The maximal design launch speed of projectiles was 100 m/s. The projectile velocity could be adjusted with the pressure in high-pressure chamber 3. When the projectile was launched into the water tank, the projectile was surrounded by supercavitation due to the high speed of the projectile.



1-high pressure nitrogen cylinder, 2-trolley rail, 3-high pressure cylinder, 4-solenoid valve, 5-pipe-valve connector, 6-trolley bracket, 7-launch tube, 8-projectile, 9-experimental water tank, 10-observation windows, 11-light source, 12-high-speed camera, 13-laptop.

Figure 1. Schematic diagram of the horizontal supercavitation experiment device.

The movement of the supercavitating projectile in the water tank was recorded with a FASTCAM SA5 high-speed camera of Photron Company, Japan. The light source required for photography was provided by three 1000 W lamps. The shooting rate of the camera was 5000 frames per second. More detailed parameters and structure of the experimental device can be found in the previously published literature [30].

The projectiles used in the experiment were all cylindrical with 6 mm diameter and 48 mm length. All of the projectiles were produced with an aluminum–magnesium alloy, and the material density was 2.72 g/cm^3 . Two different surface coatings were coated onto the surface of projectiles: one hydrophobic and one hydrophilic coating. The hydrophobic one was a water-based silicone coating with a contact angle of $100 \pm 5^\circ$, and the hydrophilic one was a gypsum coating with a contact angle of $36 \pm 5^\circ$.

According to the photos taken with the high-speed camera, the contour of the supercavitation on the projectile at different times can be measured. Figure 2 shows a schematic diagram of the measurement of the cavitation profile of the projectile. Since the taken pictures were refracted by plexiglass air or plexiglass water, the accuracy of the measurements had to be estimated. Relevant studies showed that the relative error caused by refraction in measurement is about 0.3~0.6% (Yuan et al. [31]).

The velocity of the projectile can be calculated according to the displacement difference and the time difference between the positions of the projectile in two different frames. In order to reduce the error, projectile velocities v_i' and v_i'' were first calculated with the left and right reference planes, respectively. Then, average value \bar{v}_i was taken as the velocity of the projectile. The schematic diagram of displacement measurement is shown in Figure 3. The formula for calculating the velocity of the projectile is as follows:

$$v_i' = -k \frac{x_i' - x_{i+1}'}{\Delta t} \quad (1)$$

$$v_i'' = k \frac{x_{i+1}'' - x_i''}{\Delta t} \tag{2}$$

$$\bar{v}_i = \frac{v_i' + v_i''}{2} \tag{3}$$

where Δt is the time interval between two adjacent photos, k is the ratio of the actual displacement of the projectile to the displacement on the photo.

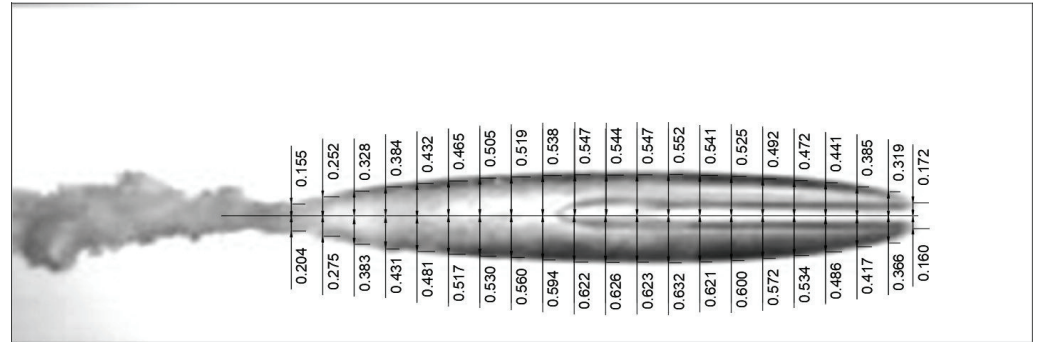


Figure 2. Measurement of cavitation profile.

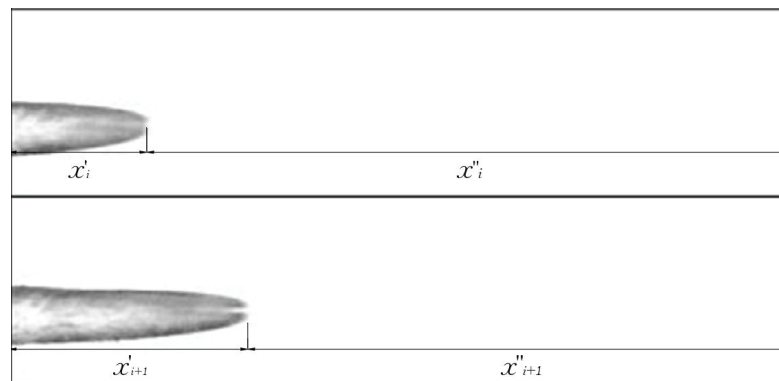


Figure 3. Schematic diagram of displacement measurements of the projectile.

In this paper, the supercavitation flow of the projectile is studied at four different water depths: 3.33D, 6.67D, 16.7D, and 33.3D, where D is the diameter of the projectile. All projectiles were horizontally fired into the water. In this paper, the cavitation number was calculated as follows:

$$\sigma = \frac{p_\infty - p_v}{\frac{1}{2} \rho_l v_\infty^2} \tag{4}$$

where p_∞ is the atmospheric pressure, p_v is the saturated vapour pressure at 20 °C, ρ_l is the liquid water density, and v_∞ is the initial speed of the projectile. The coefficient of the drag force was calculated with the following expression:

$$C_D = \frac{F_D}{\frac{1}{2} \rho_l v^2 A_0} \tag{5}$$

where F_D is the drag force, v is the local velocity of the projectile, and A_0 is the cross area of the projectile.

3. Experimental Results and Discussions

3.1. Influence of Surface Coating on the Supercavitation Characteristics

In this paper, four cases of different water depth were studied: 3.33D, 6.67D, 16.7D, and 33.3D. The photos taken in the experiment show that the horizontal motion of the

projectile did not affect the free surface under the three water depth conditions of 6.67D, 16.7D and 33.3D, that is, it did not deform the free surface, while the movement of the projectile in the water depth of 3.33D deformed the free surface. Therefore, in this part, only the supercavitation evolution under the two typical conditions of 3.33D and 16.7D is given, which is defined as the near free surface condition (3.33D) and the deep-water condition (16.7D).

3.1.1. Near Free Surface (3.33D Water Depth)

At this water depth, since the distance between the horizontal motion position of the projectile and the free surface was small, the moving projectile affected the shape of the free surface; correspondingly, the supercavitation around the projectile was also affected by the free surface.

Figure 4 shows the supercavitation evolution of the projectile with hydrophobic coating at the water depth 3.33D. The projectile was horizontally launched into the water tank. The time interval between two adjacent photos was 1 ms.

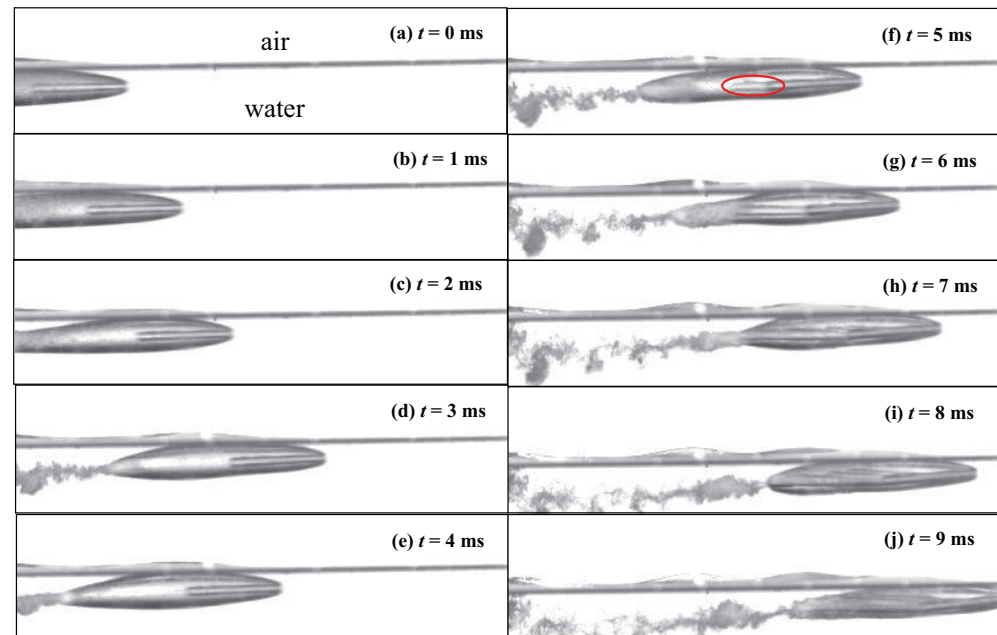


Figure 4. Supercavitation evolution of the projectile with hydrophobic coating at 3.33D water depth ($\Delta t = 1$ ms, $V_0 = 31.8$ m/s).

Figure 4a shows the deformation of the free surface, and the deformation of the free surface lagged the position of the head of the projectile. In the entire observed range, the deformation of the free surface was wavy, and the vertical water fins observed by Shi et al. [10] did not appear for this case.

In Figure 4a, the projectile was wrapped by the supercavitation. The contour of the supercavitation was asymmetric along the axis of the projectile, and the lower contour of the supercavitation was smaller than the upper contour. The reasons may have been as follows: on the one hand, in the gravitational field, cavitation was affected by upward buoyancy; on the other hand, because the projectile moved near the free surface, the upper cavity could expand by changing the shape of the free surface.

In Figure 4d, the velocity of the projectile was reduced by 20%, relative to the initial velocity; at that time, the cavitation collapsed at the tail, and the size of cavitation decreased. Figure 4f shows that a scratch appeared on the wall of the cavitation, as indicated by the red ellipse, which may have been caused by the contact between the tail of the projectile and the wall of the cavitation. Figure 4d–h show that the tail of the supercavitation continually collapsed. At the downstream flow field of the projectile, there were obvious shedding

cavity clusters and wake. Figure 4i shows that the entire cavitation around the projectile became opaque and unstable, and the collapse of the entire cavitation could be predicted. Figure 4j shows that the whole supercavitation around the projectile collapsed as predicted.

In addition, the projectile ran stably in the whole process. Figure 4a–d shows that the projectile moved completely parallel to the free surface. In Figure 4f, the projectile was slightly deflected. At that time, the tail of the projectile came into contact with the cavitation boundary, as marked by the red circle in Figure 4f. After that moment, the tail of the projectile stayed into contact with the cavitation wall, and the projectile continued to deviate from the original trajectory. In Figure 4i, the deflection angle between the axis of the projectile and the free surface is 2.5° .

Figure 5 shows the supercavitation evolution of the projectile with hydrophilic coating near the free surface. The initial velocity of the projectile in Figure 5 (37.1 m/s) was higher than that in Figure 4 (31.8 m/s). If the surface coating of the projectile was the same, the cavitation profile in Figure 5 was larger than that in Figure 4 because of the difference in velocity. However, comparing Figures 4 and 5 shows that the outline size of the supercavitation around the hydrophilic coated projectile was smaller than that of the hydrophobic coating.

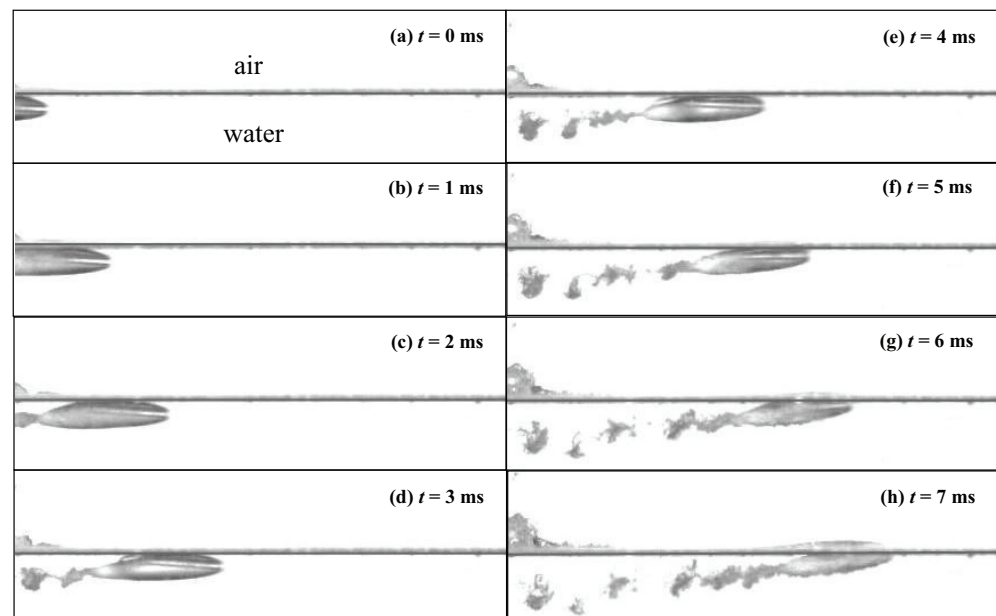


Figure 5. Supercavitation evolution of the projectile with hydrophilic coating at 3.33D water depth ($\Delta t = 1$ ms, $V_0 = 37.1$ m/s).

The influence of hydrophilic projectile on free surface is different from that of hydrophobic projectile. Figure 5c–f show the splash phenomenon on the left side of the picture, but no obvious deformation can be observed on the free surface above the projectile. In Figure 5g, the head of the projectile was close to the free surface, and at that time, the free surface above the projectile rose. Figure 5h shows the projectile starting to come out of the water.

Figure 5 shows that the hydrophilic coated projectile was unstable during the whole movement process. When the projectile entered the observation window, it deflected clockwise. Figure 5b–e shows that the deflection angle of the projectile is negative (Convention: counterclockwise is positive, clockwise is negative). In Figure 5f the deflection angle was approximately zero, that is, at that time, the projectile deflected counterclockwise. In Figure 5g, the deflect angle was already positive and the head of the projectile came into contact with the free surface. In Figure 5h, the projectile inclined out of the water. The experiment for every condition was repeated 5 times in order to obtain reliable conclusions.

Repeated experiments showed that the stability of hydrophilic projectiles was worse than that of hydrophobic ones.

3.1.2. Deep Water (16.7D Water Depth)

Figure 6 shows the evolution process of supercavitation of hydrophobic coated projectile in 16.7D water depth. The time interval between two adjacent photos is 1 ms, too. The initial velocity of the projectile is 38.3 m/s. When the projectile completely appeared in the observation window, it was wrapped by supercavitation (Figure 6b). The supercavitation contour was basically symmetrical along the axis of the body.

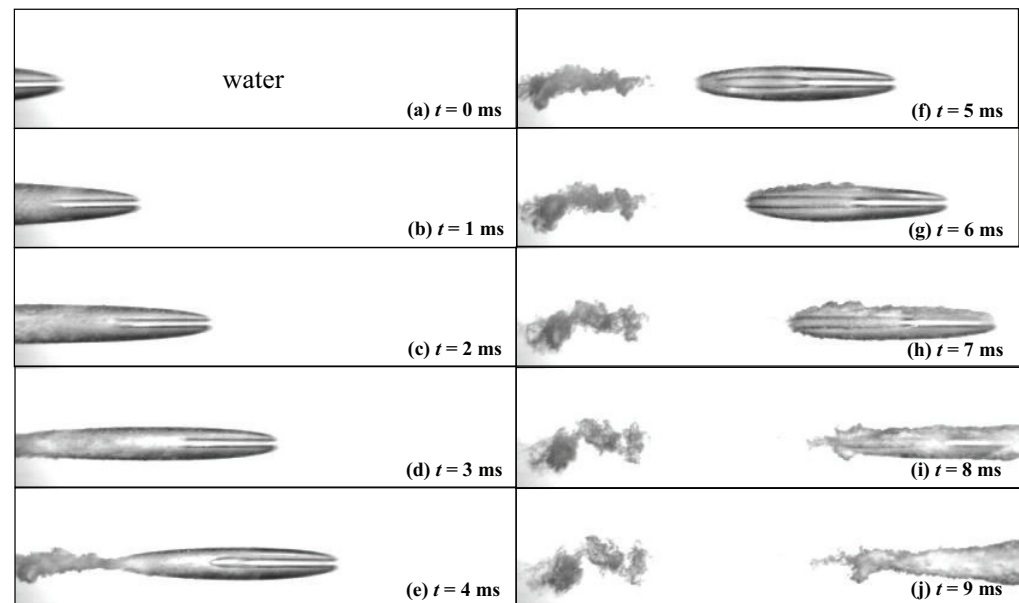


Figure 6. Supercavitation evolution of the projectile with hydrophobic coating under the water depth of 16.7D ($\Delta t = 1$ ms, $V_0 = 38.3$ m/s).

When the projectile moved forward, the velocity of the projectile decreased due to the drag force in the water. The length and diameter of the cavitation also decreased when comparing Figure 6d,e. In Figure 6g, the velocity of the projectile body dropped to 28 m/s. At that time, the upper wall of the cavitation is already disturbed while the lower wall is relatively stable, which may have been due to Reyleigh–Taylor instability. In Figure 6h, the entire upper boundary began to fluctuate, which means that the entire supercavitation was unstable. In Figure 6i, the cavitation on the projectile simultaneously collapsed from the head and tail.

Figure 7 shows the evolution process of supercavitation of hydrophilic coated projectile at the same water depth. The initial velocity of the projectile was almost the same as that in Figure 6, which is 38.4 m/s.

Comparing Figure 7 and Figure 6, the supercavitation in Figure 6 was relatively smooth and transparent, while the supercavitation interface in Figure 7 was opaque and rough. In addition, the size of the supercavitation profile of the hydrophobic projectile was larger than that of hydrophilic projectile, which is easier to see in Figures 8 and 9. In Figure 7g, the entire cavitation interface around the projectile fluctuated and was unstable, and in Figure 7h the entire cavitation collapsed.

In Figure 6, the projectile with hydrophobic coating almost moves parallel to the free surface, while the deflection angle of the projectile with hydrophilic coating is larger than 8° counterclockwise in Figure 7j. That is, for this case, the ballistic stability of hydrophobic projectile was better than that of hydrophilic projectile, too.

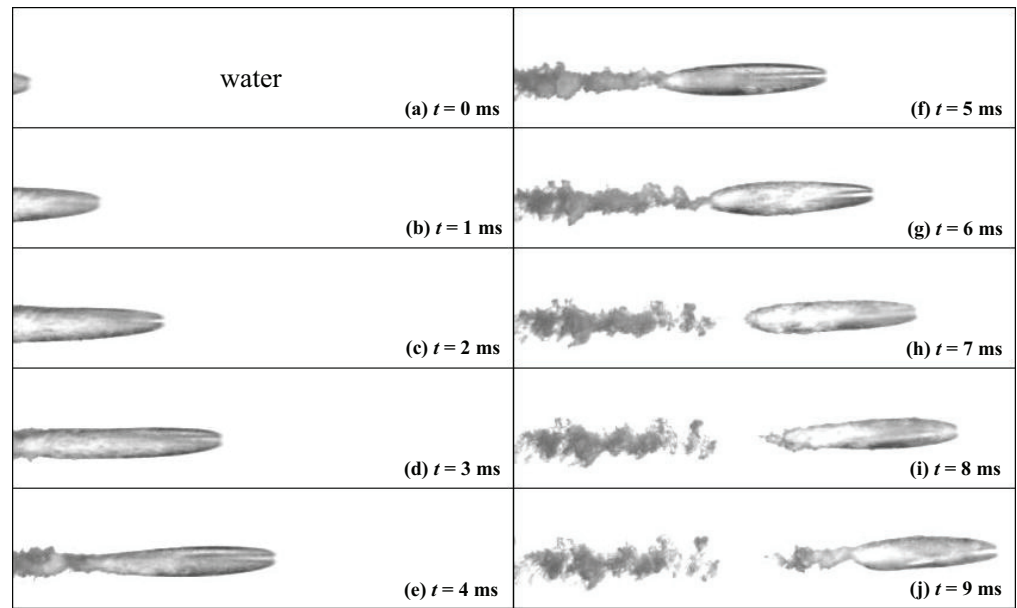


Figure 7. Supercavitation evolution of the projectile with hydrophilic coating under the water depth of 16.7D ($\Delta t = 1$ ms, $V_0 = 38.4$ m/s).

3.1.3. Supercavitation Characteristics under Different Conditions

Figures 8 and 9 show the change in the length and diameter of the cavitation with cavitation numbers for four cases. The length and the diameter of the cavitation are measured three times in order to reduce the uncertainty of the measurement. The length and diameter of the cavitation are nondimensionalized by the diameter of the projectile. The abscissa is the cavitation number, which was calculated with Equation (4). Figures 8 and 9 show that both the length and diameter of the cavity decreased with the increase in cavitation number, that is, the size of the cavity decreased with the increase in cavitation number.

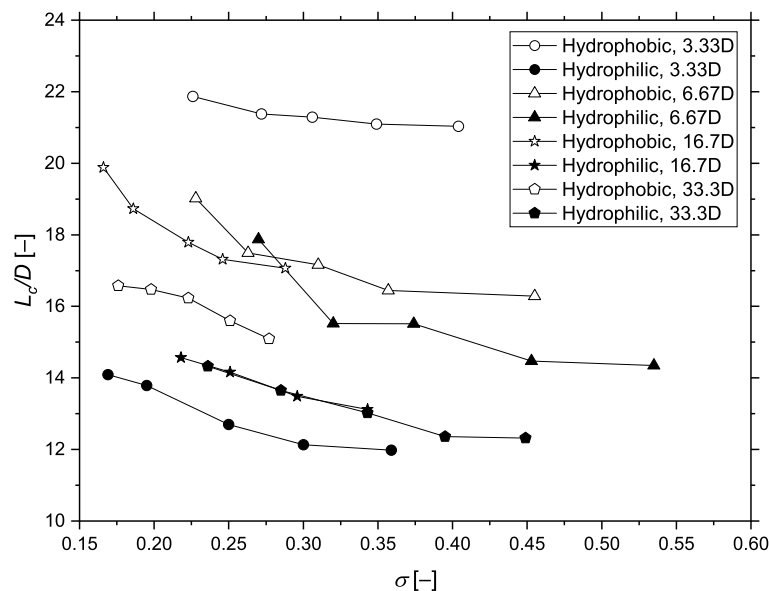


Figure 8. Relationship between dimensionless cavitation length and cavitation number.

Figure 8 shows that the cavitation length of hydrophobic projectile was larger than that of hydrophilic projectile for the case of the same water depth. At the same cavitation number, the length of cavitation decreased with the increase in water depth (except the case of 3.33D with the hydrophilic coating). Near the free surface (3.33D water depth),

the cavitation length on the hydrophobic projectile was much longer than that on the hydrophilic one, which may have mainly been due to the fact that the position of the projectile is close to the free surface, and the cavitation of the hydrophobic projectile could expand towards the free surface. However, for the hydrophilic projectile, the expansion of the cavity toward the free surface was not observed.

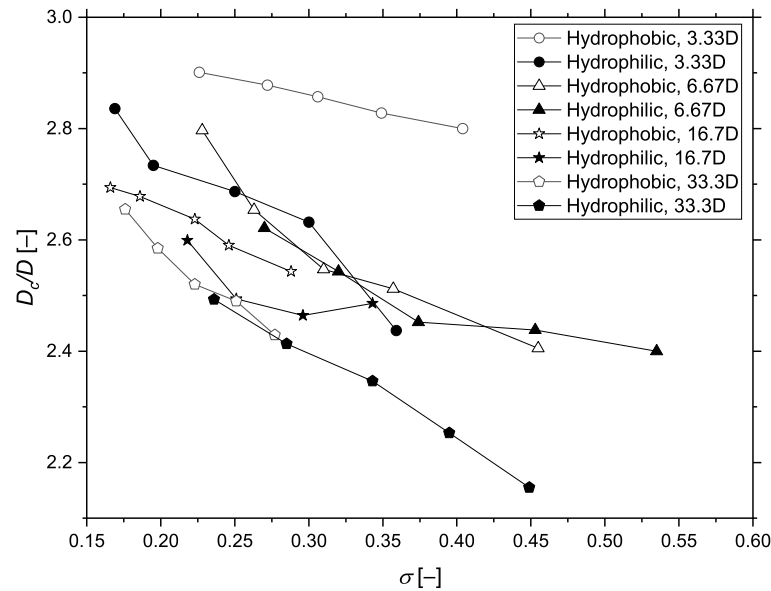


Figure 9. Relationship between dimensionless cavitation diameter and cavitation number.

Similarly, in Figure 9, for the same water depth, the cavitation diameter of the hydrophobic projectile was larger than that of the hydrophilic projectile. With the increase in water depth, the diameter of the cavity also decreases like the change rule of the cavitation length with water depth in Figure 8, which was consistent with the findings of Shi et al. [10].

Figure 10 shows the comparison of cavitation profile at water depths of 3.33D and 16.7D at a certain cavitation number. The abscissa and ordinate are the dimensionless length and diameter of the cavity, respectively. Obviously, the cavitation contour inclined upward, that is, to the free surface, in the 3.33D condition, while in the 16.7D condition, the cavitation contour was basically axisymmetric.

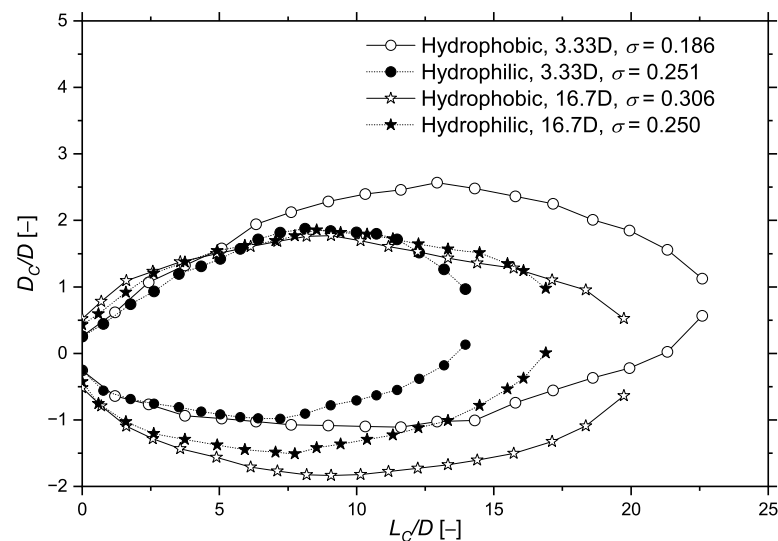


Figure 10. Comparison of cavitation profile.

In Figure 10, under the 16.7D condition, the cavitation number of the hydrophilic body was less than that of the hydrophobic body, but the cavitation size of the hydrophilic body was still smaller than that of the hydrophilic body. Cavitation size increases with the decrease in cavitation number. This also shows that, at the same cavitation number, the cavitation size of hydrophobic projectile must be larger than that of hydrophilic projectile.

3.2. Influence of Surface Coating on the Hydrodynamic Properties of the Projectile

The hydrodynamic characteristics of the projectile were closely related to the supercavitation flow field around the body. The influence of different coatings on the hydrodynamic characteristics of the projectile is discussed below.

Figure 11 shows the change of the projectile velocity with time for both hydrophilic and hydrophobic coatings at different water depths. The velocity was nondimensionalized by the initial velocity of the projectile under different conditions.

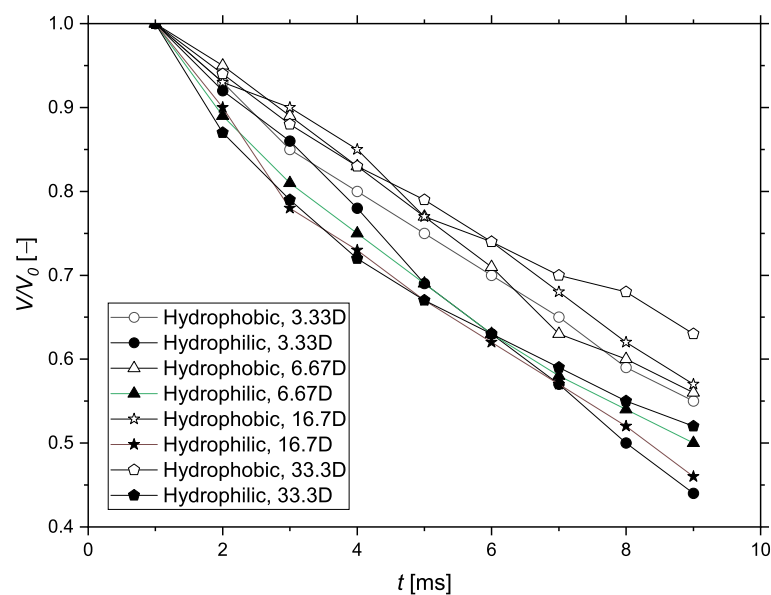


Figure 11. Variation in the dimensionless velocity of the projectile with time under different water depths.

Figure 11 shows that the projectile velocity with the hydrophilic coating decreased faster than that with the hydrophobic coating for four conditions with different water depth. At the water depth of 3.33D, the decrease in the velocity of the hydrophilic-coated projectile was about 56% after 8 ms, while the decrease in the hydrophobic-coated projectile was about 45%. At the water depth of 16.7D, after 8 ms, the decrease velocity for the hydrophilic- and hydrophobic-coated projectile was about 54% and 43%, respectively. That is, the velocity decay of hydrophobic projectiles is about 20% slower than that of hydrophilic ones. This means that the drag force on the projectile with hydrophobic coating was smaller than that on the hydrophilic-coated projectile, which could be verified with the figure of the drag force coefficient versus cavitation number.

Figure 12 shows the relationship between the drag coefficient and the cavitation number for different conditions. The calculation of the cavitation number and drag coefficient is given in Equations (4) and (5). Figure 12 shows that, for every condition, the drag coefficient of the projectile increased with the increase in cavitation number, while the drag coefficient of the hydrophobic-coated projectile was lower than that of the hydrophilic coating in every water depth. For projectiles with different coatings, even though the cavitation number was the same, the drag coefficient on the projectiles was also different. This was due to the different shapes of the cavitation wrapped on different coated projectiles. Under the working conditions of 6.67D, 16.7D, and 33.3D, the drag coefficient of hydrophobic projectile could be reduced by 20–40% at a certain cavitation number compared with that

of hydrophilic projectile. Near the free surface, the reduction in the drag coefficient due to the hydrophobic effect is slightly smaller compared with the other conditions of water depths. In the studied working conditions, at the water depth of 33.3D and $\sigma = 0.34$, the drag reduction in hydrophobic projectile reaches its maximum, about 40%, compared with that of hydrophilic projectile.

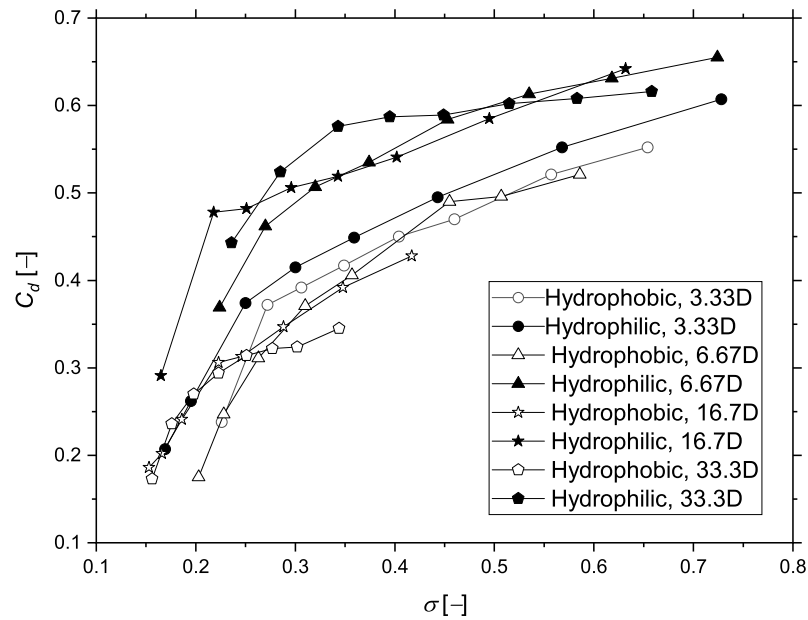


Figure 12. Relationship between drag coefficient and cavitation number for different conditions.

In order to study the effect of surface coating on the ballistic stability of the projectile, Figures 13 and 14 show the relationship between the deflection angle of the projectile and the deflection angular rate of the projectile with time under different working conditions. The counterclockwise deflection was positive and the clockwise deflection was negative. The error of the deflection angle was about 0.2° .

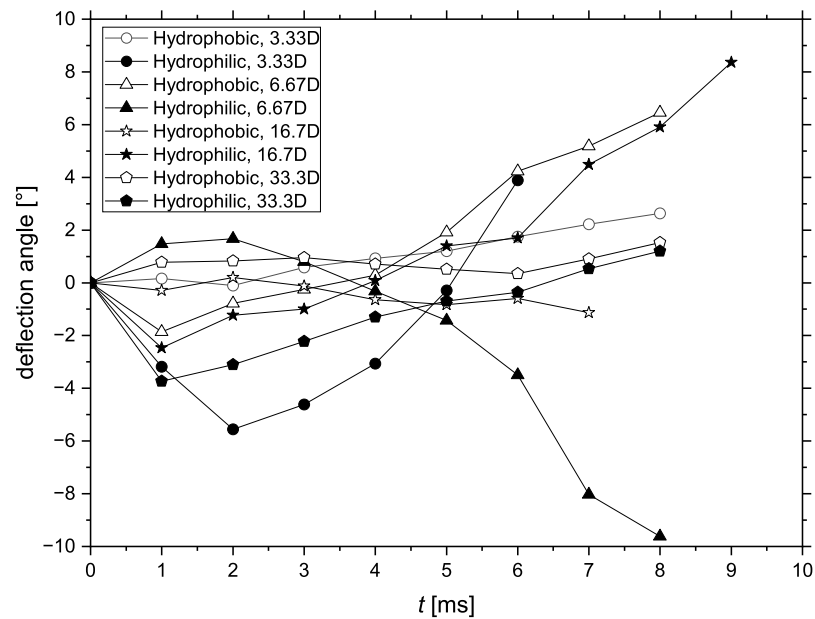


Figure 13. Variation in deflection angle of the projectile with time under different working conditions.

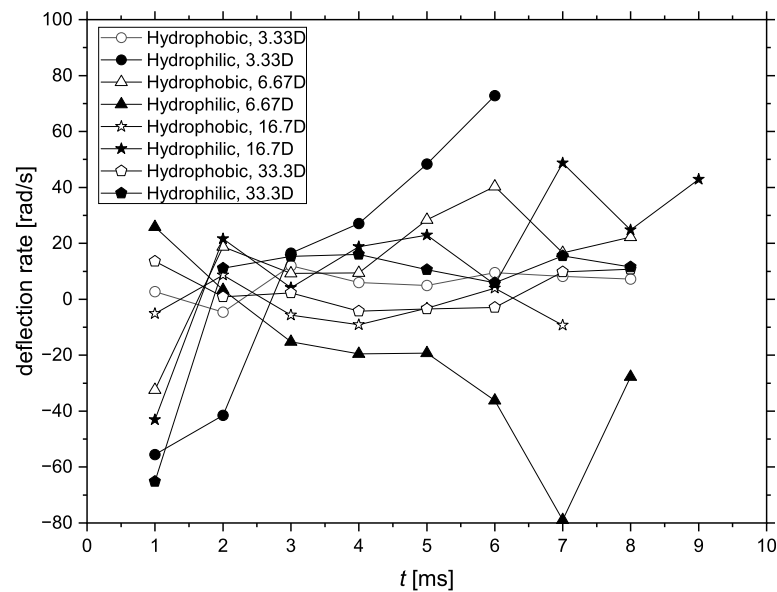


Figure 14. Relationship between the deflection angular rate of the projectile and time under different working conditions.

For the projectile with hydrophilic coating, at the water depth of 3.33D, the projectile first deflected clockwise and then counterclockwise. At $t = 6$ ms, the deflection angle in the reverse direction was about 4° . Although this deflection angle of the projectile was not large, the deflection angular rate of the projectile at this time was very large, larger than 70 rad/s at $t = 6$ ms. That is, the ballistics of the projectile was not stable under this working condition, which can also be seen in Figure 5. For the other two operating conditions (6.67D and 16.7D), the deflection angle of the projectile was up to greater than 8° within the observation range. At that time, the deflection angular rate of the projectile was also relatively large, larger than 20 rad/s at $t = 8$ ms for both cases. That is, for these two cases, the ballistics of the projectile was also not stable. For the case of 33.3D, the projectile first deflected about 4° clockwise, and then deflected counterclockwise due to the interaction between the tail of the projectile and upper boundary of the supercavitation (no figure). Figure 14 shows that, from $t = 2$ to $t = 8$ ms, the deflection angular rate of the projectile remained at a relatively stable lower value, and the projectile ran relatively stable.

For hydrophobic projectiles, in the cases of 3.33D, 16.7D, and 33.3D, the deflection angles of the projectiles were all small, about 2° . For the case of 6.66D, the deflection angle of the projectile reached about 6° at $t = 8$ ms. However, Figure 14 shows that the deflection angular rate of the projectile decreased from $t = 6$ ms to $t = 8$ ms.

In summary, for the two surface coatings studied in this paper, the ballistic stability of the hydrophobic projectile was better than that of the hydrophilic one for different water depth conditions, which was confirmed with repeated measurements for each case.

4. Discussion

In this paper, the effects of two kinds of surface coatings (one hydrophilic, and the other hydrophobic) on the supercavitation flow field and hydrodynamic characteristics of projectiles were studied. The properties of coatings had obvious effects on cavitation size, drag force on projectiles, and ballistic stability. Due to the limited research objects in this paper, further research is needed on the quantitative influence of hydrophilic, hydrophobic, and superhydrophobic coatings with more contact angles.

In addition, with the decrease in water depth, both the length and diameter of the cavitation increased. This conclusion is consistent with the research results of Shi et al. [10]. However, the research of Faltinsen and Semenov [8] found that the length of the cavitation decreased, and the diameter of the cavitation increased with the decrease in water depth,

which was inconsistent with the result in this paper. The cavitating flows in both this paper and that of Shi et al. [10] were unsteady, while Faltinsen and Semenov [8] studied steady cavitating flow. Moreover, Faltinsen and Semenov [8] did not consider the viscous effect of the fluid. In addition, the head shape of the object affected the shape of the cavitation. In the research of Faltinsen and Semenov [8], the cavitating flow around a hydrofoil was considered, while in the research of Shi et al. [10] and this paper, the moving body was a cylinder. However, the change in cavitation size with water depth should be further studied in detail.

5. Conclusions

In this paper, the supercavitation characteristics and hydrodynamics of a projectile with hydrophobic and hydrophilic coatings were studied experimentally. The experiments were carried out under four water depths (3.33D, 6.67D, 16.7D, and 33.3D).

The experimental results show that the length and the diameter of the supercavitation of the projectile with the hydrophobic coating were larger than those with the hydrophilic coating, which was probably due to the difference of the contact angles under different surface coatings. The length and the diameter of the supercavitation increased with the decrease in the water depth for the projectile with hydrophobic coating. The drag force coefficient of the hydrophobic projectile was obviously smaller than that of the hydrophilic one at the same cavitation number and water depth. Under the working conditions of 6.67D, 16.7D, and 33.3D, the drag coefficient of hydrophobic projectile could be reduced by 20–40% at a certain cavitation number compared with that of hydrophilic projectile. The velocity decay of the hydrophobic projectile was obviously slower than that of hydrophilic projectile.

In addition, the ballistic stability of the projectile with the hydrophobic coating was better than that with the hydrophilic coating. The hydrophobic projectile could basically follow the original trajectory, while the hydrophilic projectile easily deviated from the original path.

The effect on the free surface with different coatings was also different. In our experiment, the formation of the free surface for the hydrophobic body showed smooth waves, and no vertical water fin appeared.

Author Contributions: Conceptualization, H.J.; Methodology, H.J.; Software, R.X.; Experiment, R.X. and Y.Z.; Data processing, R.X. and Y.Z.; Writing—original draft, Y.Z.; Writing—review & editing, H.J. All authors have read and agreed to the published version of the manuscript.

Funding: This research work was financially supported by the National Natural Science Foundation of China (Grant No. U21A20126) and Zhejiang Sci-Tech University (No. 0803609-Y).

Data Availability Statement: Not applicable.

Acknowledgments: The authors would like to thank the National Natural Science Foundation of China for the financial support. The authors would also like to thank Honghui Shi for his help and guidance.

Conflicts of Interest: The authors declare no conflict of interest. The funders had no role in the design of the study; in the collection, analyses, or interpretation of data; in the writing of the manuscript; or in the decision to publish the results.

References

1. Logvinovich, G.V. *Hydrodynamics of Free-Boundary Flows*, 1st ed.; IPST Press: Jerusalem, Israel, 1972.
2. Waugh, J.G.; Stubstad G.W. *Hydroballistics Modeling*, 1st ed.; US Government Printing House: Washington, DC, USA, 1975.
3. Vlasenko, Y.D. Experimental investigations of high-speed unsteady supercavitating flows. In Proceedings of the 2th International Symposium on Cavitation, Grenoble, France, 7–10 April 1998; pp. 39–44.
4. Hrubes, J.D. High-speed imaging of supercavitating underwater projectiles. *Exp. Fluids* **2001**, *30*, 57–64. [[CrossRef](#)]
5. Shi, H.H.; Kume, M. An experimental research on the flow field of water entry by pressure measurements. *Phys. Fluids* **2001**, *13*, 347–349. [[CrossRef](#)]
6. Franc, J.P.; Michel, J.M. *Fundamentals of Cavitation*, 1st ed.; Springer Science & Business Media: Berlin/Heidelberg, Germany, 2005; pp. 60–92.

7. Amromin, E. Analysis of body supercavitation in shallow water. *Phys. Fluids* **2007**, *34*, 1602–1606. [[CrossRef](#)]
8. Faltinsen, O.M.; Semenov, Y.A. The effect of gravity and cavitation on a hydrofoil near the free surface. *J. Fluid Mech.* **2008**, *597*, 371–394. [[CrossRef](#)]
9. Wang, Y.; Wu, X.; Huang, C.; Wu, X. Unsteady characteristics of cloud cavitating flow near the free surface around an axisymmetric projectile. *J. Multiph. Flow* **2016**, *85*, 48–56. [[CrossRef](#)]
10. Shi, H.-H.; Zhou, Y.-J.; Jia, H.-X.; Zhu, B.-B. The Effects of Water Depth and Length-to-diameter Ratio on Drag Coefficient and Cavity Shape of Underwater Supercavitating Projectiles. *Acta Armamentarii* **2016**, *37*, 2029–3035.
11. Min, T.; Kim, J. Effects of hydrophobic surface on skin-friction drag. *Phys. Fluids* **2004**, *16*, L55–L58. [[CrossRef](#)]
12. Aljallis, E.; Sarshar, M.A.; Datla, R.; Sikka, V.; Jones, A.; Choi, C.H. Experimental study of skin friction drag reduction on superhydrophobic flat plates in high Reynolds number boundary layer flow. *Phys. Fluids* **2013**, *25*, 025103. [[CrossRef](#)]
13. Park, H.; Sun, G. Superhydrophobic turbulent drag reduction as a function of surface grating parameters. *J. Fluid Mech.* **2014**, *747*, 722–734. [[CrossRef](#)]
14. Xu, M.; Grabowski, A.; Yu, N.; Kerezyte, G.; Lee, J.W.; Pfeifer, B.R. Superhydrophobic drag reduction for turbulent flows in open water. *Phys. Rev. Appl.* **2020**, *13*, 034056. [[CrossRef](#)]
15. Xu, M.; Arihara, B.; Tong, H.; Yu, N.; Ujiie, Y.; Kim, C.J. A low-profile wall shear comparator to mount and test surface samples. *Exp. Fluids* **2020**, *61*, 82. [[CrossRef](#)]
16. Xu, M.; Yu, N.; Kim, J. Superhydrophobic drag reduction in high-speed towing tank. *J. Fluid Mech.* **2021**, *908*, A6. [[CrossRef](#)]
17. Leger, A.T.; Ceccio, S.L. Examination of the flow near the leading edge of attached cavitation. Part 1. Detachment of two-dimensional and axisymmetric cavities. *J. Fluid Mech.* **1998**, *376*, 61–90. [[CrossRef](#)]
18. Kawakami, D.T.; Fuji, A.; Tsujimoto, Y.; Arndt, R.E.A. An Assessment of the Influence of Environmental Factors on Cavitation Instabilities. *ASME J. Fluids Eng.* **2008**, *130*, 031303. [[CrossRef](#)]
19. Kim, J.; Lee, J.S. Numerical study of cloud cavitation effects on hydrophobic hydrofoils. *Int. J. Heat Mass Transf.* **2015**, *83*, 591–603. [[CrossRef](#)]
20. Mineshima T.; Onishi K.; Miyagawa K. Flow field and cavitation characteristics of hydrofoils coated with hydrophilic and hydrophobic polymers. *IOP Conf. Ser. Earth Environ. Sci.* **2019**, *240*, 062055. [[CrossRef](#)]
21. Onishi K.; Matsuda K.; Miyagawa K. Influence of hydrophilic and hydrophobic coating on hydrofoil performance. In Proceedings of the International Symposium on Transport Phenomena and Dynamics of Rotating Machinery (ISROMAC 2017), Maui, HI, USA, 16–21 December 2017.
22. Ueda, Y.; Tanaka, M.; Uemura, T.; Iguchi, M. Water entry of a superhydrophobic low-density sphere. *J. Vis.* **2010**, *13*, 289–292. [[CrossRef](#)]
23. Duclaux, V.; Caillé, F.; Duez, C.; Ybert, C.; Bocquet, L.; Clanet, C. Dynamics of transient cavities. *J. Fluid Mech.* **2007**, *591*, 1–19. [[CrossRef](#)]
24. Aristoff, J.M.; Bush, J.W.M. Water entry of small hydrophobic spheres. *J. Fluid Mech.* **2009**, *619*, 45–78. [[CrossRef](#)]
25. Speirs, N.B.; Mansoor, M.M.; Belden, J.; Truscott, T.T. Water entry of spheres with various contact angles. *J. Fluid Mech.* **2019**, *862*, 45–78. [[CrossRef](#)]
26. Zhang, Q.; Zong, Z.; Sun, T.Z.; Chen, Z.Y.; Li, H.T. Experimental study of the evolution of water-entry cavity bubbles behind a hydrophobic sphere. *Phys. Fluids* **2020**, *32*, 062109. [[CrossRef](#)]
27. Li, D.; Zhao, X.; Kong, D.; Shentu, J.; Wang, G.; Huang, B. Numerical investigation of the water entry of a hydrophobic sphere with spin. *Int. J. Multiph. Flow* **2020**, *126*, 103234. [[CrossRef](#)]
28. Güzel B.; Korkmaz F.C., Experimental investigation of water entry of bodies with constant deadrise angles under hydrophobic effects. *Exp. Fluids* **2021**, *62*, 107. [[CrossRef](#)]
29. Guzel, B.; Korkmaz, F.C. Experimental investigation of water exit under hydrophobic effects. In Proceedings of the ASME 2016 35th International Conference on Ocean, Offshore and Arctic Engineering, Busan, Republic of Korea, 19–24 June 2016; pp. 1–6.
30. Zhou, S.Y. The Generation and Fluid Mechanics Mechanism of Horizontally Moving Supercavities. Master's Thesis, Zhejiang Sci-Tech University, Hangzhou, China, 2013.
31. Yuan, X.L.; Zhang, Y.W.; Liu, L.H. Research on measurement and analysis method of cavitation shape. *Exp. Mech.* **2006**, *21*, 215–219.